Experimental study on the capillary water absorptivity of an aerogel-based coating mortar under subsequent drying and wetting cycles

Experimental study on the capillary water absorptivity of an aerogel-based coating mortar under subsequent drying and wetting cycles

Experimental study on the capillary water absorptivity of an aerogel-based coating mortar under subsequent drying and wetting cycles

A N Karim[1], **A Sasic Kalagasidis**[1] **and P Johansson**[1]

[1]Department of Architecture and Civil Engineering, Chalmers University of Technology, Sweden

E-mail: ali.karim@chalmers.se

Abstract. Aerogel-based coating mortars with thermal conductivities ranging from 30 to 50 mW/(m·K) are an emerging type of thermal insulation coating mortar. They are intended for retrofitting uninsulated building envelopes due to their thermal performance which is comparable to conventional thermal insulation materials such as mineral wool. Meanwhile, their long-term hygrothermal performance and the reliability of the material properties are not fully demonstrated since these normally are declared based on single-cycle laboratory measurements. This paper presents laboratory measurements to determine the capillary water absorptivity of a commercial aerogel-based coating mortar after three consecutive wetting and drying cycles. The effect of the chosen drying (elevated versus room temperature) and sealing condition (sealed versus unsealed samples) on the measurement results were also assessed. The results show that the capillary water absorptivity of the samples increased after each repeated wetting and drying cycle regardless of the drying and sealing conditions. After three cycles, the measured capillary water absorption was more than five times higher than the initial measurement. Future research should investigate the causes of the observation and whether it applies to other aerogel-based coating mortars.

1. Introduction

Aerogel-based coating mortars (ACMs) are a new type of multifunctional and energy-efficient wall finishes for both internal and external applications, with thermal conductivities ranging from 30 to 50 mW/(m·K) [1]. These values are comparable to the thermal conductivities of traditional thermal insulation materials like mineral wool and polystyrene, and more than ten times lower than the value for conventional coating mortars. As a result, when energy retrofitting uninsulated building envelopes, ACMs can introduce new technical solutions. According to the review conducted by Karim et al. [1], research has shown that applying 15-60 mm of ACMs to uninsulated masonry walls reduced their U-values by 27-70%. Furthermore, ACMs can be used in the retrofitting of listed buildings to overcome some of the challenges associated with the preservation of character-defining elements and allowed thickness of the building envelope.

ACMs are based on a mixture of lime and white cement as binder. The aggregates typically have a high proportion (more than 50% vol-%) of hydrophobized silica aerogel granules. Aerogel is a highly porous, ultralight super insulation material with thermal conductivities ranging from 10 to 20 mW/(m·K). The final coating mixture also contain various additives such as air-entraining and water-repellent agents [1]. ACMs are vapor permeable, with a vapor permeability coefficient, μ-value (-), of 4-6, which is comparable to or lower than most conventional mortars. The low vapor permeability and water repellent properties of ACMs are important in the context of moisture-safe design, especially when retrofitting moisture-damaged structures. ACMs are highly fragile and have low mechanical strength due to their low density and high proportion of aerogel granules. Therefore, it is recommended that ACMs are used in a multi-layer wall system [1]. To improve adhesiveness, the coating system includes an undercoat layer between the substrate and the ACM. Reinforcement mortar and mesh are applied to the exterior and on top of the ACM to provide the necessary mechanical strength to the coating system. The additional coating layers combined with ACM increase the total thickness of the multilayer wall system by approximately 10 mm. Thus, for a system with 40 mm of ACM, the total thickness will be around 50 mm. For conventional mortars, the total thickness is normally less than 30 mm.

Previous research on ACMs has primarily focused on their thermal performance [1]. Despite the superior thermal performance of ACMs reported in the literature, their long-term and hygrothermal (heat and moisture) performance has not been thoroughly studied. Many commercial ACMs lack complete and reliable data on moisture-related properties such as moisture sorption isotherm with hysteresis effect, capillary water absorption coefficient, moisture-dependent thermal conductivity, and free-water saturation moisture content. The incomplete data set on the long-term hygrothermal properties of ACMs can complicate moisture risk analyses, which are commonly practiced in climates with high moisture loads on buildings. The south and west regions of Sweden, for example, have subpolar oceanic climate [2], i.e., the humid temperate climate subtype (Cfb), which is characterized by high humidity and rain throughout the year.

Previously, the long-term performance of trial mixtures of ACMs has been studied in [3–8] by means of artificial weathering cycles in laboratory [1]. Trial mixtures refer here to non-commercial mortar mixtures containing various fractions of aerogel granules prepared in the laboratory for systematic research. Only two of these studies [4,5] evaluated the long-term water absorptivity of the trial mixtures of ACMs, while the others focused on thermal and mechanical properties of the ACMs. Maia et al. [5] measured the capillary water absorptivity of ACM samples subjected to various consecutive weathering cycles in laboratory. Before and after the weathering cycles, the measured A_{cap} was around 0.8 kg/(m^2·min$^{0.5}$) [5] indicating that it was stable but high for a thermal insulation coating mortar. In another study, Sakiyama et al. [4] exposed large-scale wall prototypes of trial mixtures of ACM to severe weathering cycles in the laboratory at which the walls insulated by ACM showed signs of excessive water intrusion after the weathering cycles. In [9–15], the A_{cap} of trial mixtures of ACMs was declared in based a single round of measurement, i.e., one wetting and drying cycle, as specified in EN ISO 1015-18 [16]. The declared values in [9–15] ranged from 0.48 and 2.8 kg/(m^2·min$^{0.5}$), which are all higher than the stated requirement for thermal insulation coating mortars of less than 0.4 kg/(m^2·min$^{0.5}$) [17]. The literature review highlights that studies on the A_{cap} of ACMs are limited to a few studies that focus on trial mixtures with scattered results. The composition of commercial ACMs differ from the trial mixtures studied in [4,5,9–15]. As a result, the properties of commercial ACMs may differ from those of the studied trial mixtures.

The aim of this study is to contribute to the knowledge gap identified in the literature concerning the long-term water absorptivity of ACMs. Therefore, the capillary water absorptivity of a commercial ACM exposed to multiple subsequent wetting and drying cycles is measured in laboratory. The effect of the wetting and drying cycles is investigated by measuring the total water mass gain and A_{cap} of the ACM samples after each cycle.

2. Laboratory measurements

Figure 1 summarizes the preparation and testing procedure implemented. Four sample sets, including three identical samples each, were considered in the measurements. All samples were exposed to three wetting and drying cycles and the water mass gain (kg/m^3) due to capillary water absorption and the A_{cap} (kg/(m^2·min$^{0.5}$)) of each sample was measured.

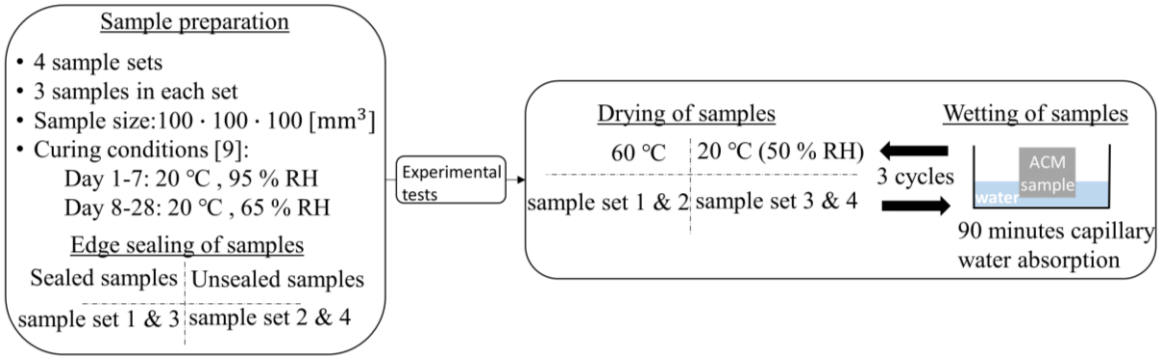

Figure 1. The experimental methodology in the study where 12 samples were produced, cured and dried under 4 different conditions.

2.1. Sample preparation

Table 1 compiles the declared material properties of the selected ACM product. The mixing procedure specified in the technical data sheet of the ACM product was used to prepare the test samples. The samples were cast and cured in accordance with EN ISO 1015-18 [16], see figure 1 and figure 2 a-c. All ACM samples were 100·100·100 mm^3, a moderate upscaling of the sample size suggested in [16]. The standard [16] and suggested sample size were originally designed for conventional coating mortars and not specifically for ACMs. In this study, multiple initial attempts to prepare prismatic samples failed. Once removing the casting form, the samples cracked, or the corners were broken into smaller pieces. The fragility and low mechanical strength of the ACM, because of its low density and high proportion of aerogel granules, were the main difficulties for creating undamaged and identical prismatic halves. To overcome these difficulties, an upscaling was made from prismatic to cubic samples. After curing, epoxy glue was used to seal all surfaces except one of the cubic samples in sample set 1 and 3. The samples in sample set 2 and 4 were kept unsealed. This deviation in sealing condition among the sample sets was to study the impact of the recommended edge sealing method, given in the standard, on the measurement results.

Table 1. The declared material properties of the studied ACM [18].

Material property	Unit	Declared value
Bulk Density (ρ)	(kg/m^3)	180
Thermal conductivity (λ)	mW/(m·K)	40
Water vapor permeability coefficient (μ-value)	-	≤ 5
Water absorption coefficient (A_{cap})	kg/(m^2·min$^{0.5}$)	≤ 0.2 (W2)
Compressive strength (σ_c)	N/mm^2	0.5 (CS I)

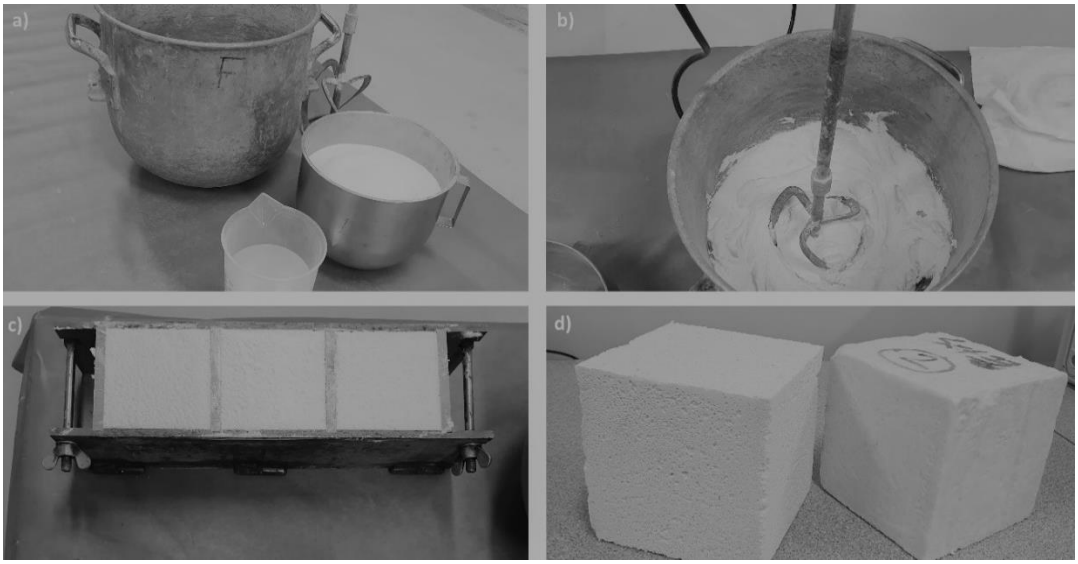

Figure 2. (a-c): Mixing and casting of fresh mortar for preparation of cubic ACM samples. (d): Hardened cubic ACM samples.

2.2. Experimental tests

As illustrated in Figure 1, the laboratory testing included three rounds of measurements, i.e., three wetting and drying cycles for each sample in all four sample sets. After each cycle, the total water mass gain (kg/m^2) was measured for 90 minutes and the A_{cap} was calculated following EN ISO 1015-18 [16]. Each cycle began with the ACM samples being dried. Sample set 1 and 2 were dried at an elevated temperature of 60±5 °C [16] in a ventilated oven. For sample set 3 and 4, drying was performed at a room temperature of 20±0.5 °C (50±2 % RH). The latter option was chosen to assess the effect of the selected drying condition on the water absorptivity measurements of the ACM samples. The drying period was terminated when each sample maintained a constant mass, as suggested in [16]. A mass change of less than 2% between two subsequent weightings within a 24-hour period was defined as constant mass.

Figure 3 depicts an example of the experimental set up used to determine the capillary water absorption of ACM samples. Each ACM sample was placed in a separate, closed container and in constant contact with water for 90 minutes. The water level in the containers was kept at a minimum of 5-10 mm [16] and the water mass gain of each ACM sample was measured after 10, 20, 45 and 90 minutes, respectively. The weighting was done using a scale of the model METTLER TOLEDO PG503-S with a resolution of 0.001 g. The A_{cap} (kg/(m^2·min$^{0.5}$)) of each sample was calculated using (1) [16]:

$$A_{cap} = 0.1 \cdot (M_2 - M_1) \quad (1)$$

Where M_2 (g) and M_1 (g) are the weights of the measured sample after 90 and 10 minutes, respectively. The measured weights for the cubic samples with a contact surface area of 100·100 mm^2 were recalculated to correspond to the same for prismatic samples with a surface area of 40·40 mm^2. This was done assuming a linear relationship between mass gain and sample contact surface area. To be noted is that the method specified in [16] for determining A_{cap}, i.e. (1), is for samples fully dried at elevated temperatures such as those in sample set 1 and 2. Therefore, for sample set 3 and 4 dried at room temperature, the changes in the water mass gain of the samples after each cycle is the parameter of interest rather than the absolute values of the calculated A_{cap}.

Figure 3. The experimental set up where each sample, placed in separate and closed container, was in contact with water with a minimum water level of 5-10 mm. The water mass gain was weighted manually by a scale for 90 minutes.

3. Results

Figure 4 presents the calculated A_{cap} for all sample sets. Figure 5 shows the measured water mass gain (kg/m^2) for 90 minutes for all sample sets (1-4). The results shown for each sample set are the average of all three samples in the sample set under consideration. The standard deviation (SD) for each measurement point was calculated using (2) and illustrated in figure 4 and figure 5.

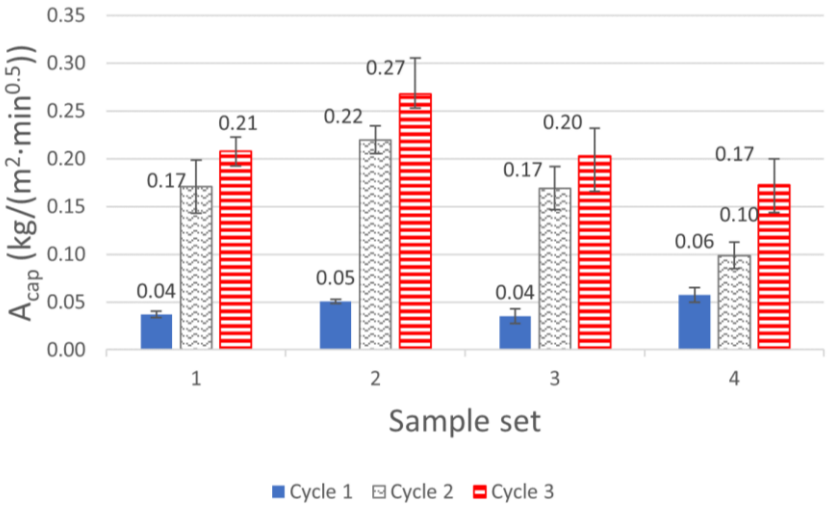

Figure 4. The calculated water absorption coefficient, A_{cap} ($kg/(m^2 \cdot min^{0.5})$), of ACM samples using (1).

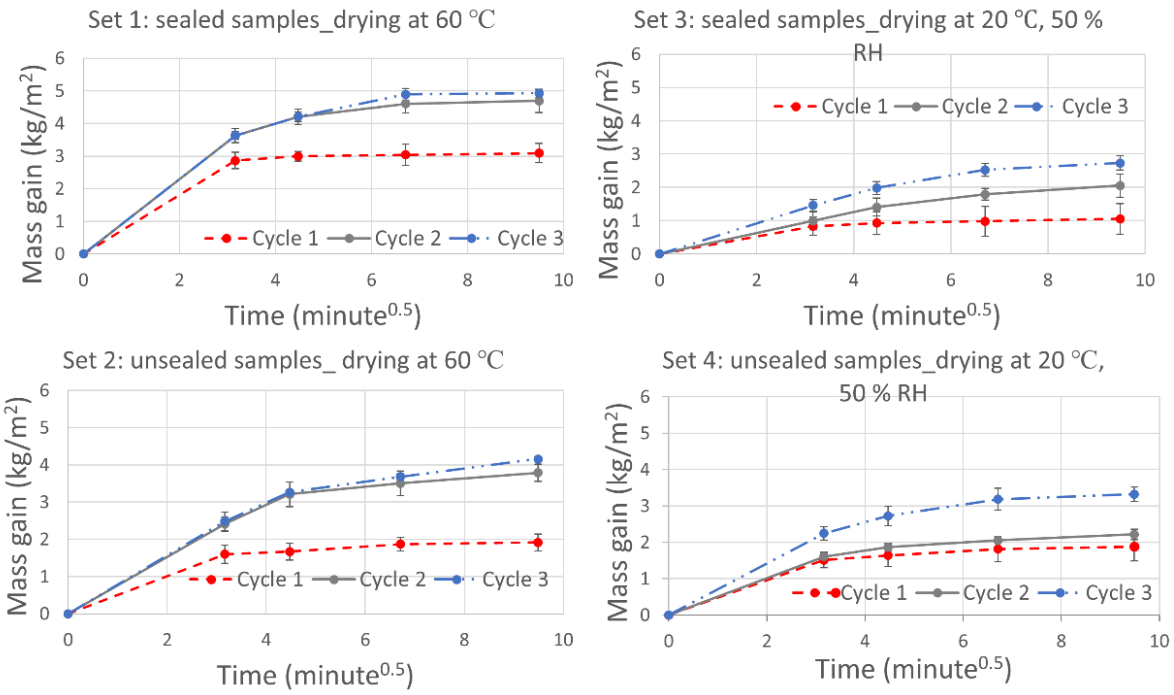

Figure 5. The measured water mass gain (kg/m^2) of ACM samples due to capillary water absorption.

$$SD = \sqrt{\frac{\sum_{i=1}^{\text{number of samples}} (\text{mean value} - \text{measured value}_i)^2}{\text{number of samples} - 1}} \quad (2)$$

The results show that after each wetting and drying cycle, both the mass gain due to capillary water absorption, and the corresponding calculated A_{cap} was increased for all sample sets. The calculated A_{cap} after the first cycle was 0.04-0.06 kg/(m^2·min$^{0.5}$) for all four sample sets. These values correspond to the lower range of the declared value for the studied ACM (less than 0.2 kg/(m^2·min$^{0.5}$)). For sample set 1, sealed and dried according to the standard [16], the A_{cap} after the second and third cycle was increased from 0.04 kg/(m^2·min$^{0.5}$) to 0.17 and 0.21 kg/(m^2·min$^{0.5}$), respectively. In other words, the water absorptivity of the samples increased more than five times between the first and third cycle. Meanwhile, the rate of increase between the second and third cycle was lower for sample set 1 and 2. Regardless of the drying and sealing conditions used, the other three sample sets showed a similar magnitude of increase. The coefficient of variance (CV) of the measurements, i.e., the relation between the calculated SD and the measured mean value for each sample set varied between 7-22 %. The CV of 22 % indicates a large variation among the measurement results in some of the sets.

When the impact of the two drying conditions (drying at 60 °C versus 20 °C) was considered, the total mass gain after three cycles was approximately 30-50 % higher for sample sets 1 and 2 fully dried at 60 °C compared to sample sets 3 and 4 dried at 20 °C. In terms of sample surface sealing (sealed versus unsealed), the difference in the total mass gain between unsealed and sealed samples was not fully clear. The total mass gain after each cycle for the unsealed samples in sample set 2 was around 20-40 % less than for the sealed sample set 1. Both sample sets were dried at 60 °C. For sample set 3 and 4 dried at 20 °C, the total mass gain for the unsealed samples in sample set 4 was approximately 30-65 % higher than the same for the sealed sample set 3. The calculated A_{cap} for the unsealed sample set 2 was on average 20-25 % higher than the same for the sealed sample set 1. Meanwhile, the calculated A_{cap} for the unsealed sample set 4 was around 15-50 % lower than the sealed sample set 3 at the second and third cycles.

4. Discussion

The measurements revealed that the water absorptivity of the ACM samples included in all four sample sets increased. This increasing trend was evident already after one extra wetting and drying cycle. While the choice of drying and sealing conditions could affect the results, they cannot be the decisive reasons for the observed increasing absorptivity of the material. The largest coefficient of variance of the measurements was 22% and expected due to the inhomogeneity of the samples, uncertainties associated with the manual weighting procedure or the accuracy of the scale. However, the measurement uncertainties could not explain the observed water absorptivity being more than five times higher after the third cycle. Possible explanations for the latter could be connected to a low mechanical strength of the material and consequentially causing micro cracking, reduced hydrophobicity, or inhomogeneous moisture distribution and pore structure of the ACM after each drying cycle. These structural changes could introduce new and different moisture flow paths in the material, resulting in higher capillary water absorption. Further experimental studies have yet to confirm these hypotheses. As stated in Section 1, previous research on this topic has been limited [4,5], and the observed phenomenon has not been reported before. While the measured A_{cap} for the commercial ACM studied here varied between 0.04-0.27 kg/($m^2 \cdot min^{0.5}$), it is still lower than the previously declared values (0.48-2.8 kg/($m^2 \cdot min^{0.5}$)) of the trial mixtures in [9–15].

In risk assessment analyses, if not taking into account the increasing water absorptivity of the ACM, an underestimation of the moisture content in the considered construction can be made along with the related moisture risks. It is worth noting that ACMs are, in practice, covered by ordinary coating mortars, as described in Section 1. Consequently, the material is normally less exposed to the same magnitude of free water absorption compared to the laboratory measurements presented. However, in case of damage and rainwater leakage through the coating mortars, an ACM may be subjected to several wetting and drying cycles over the course of its service life, potentially increasing the water absorptivity of the material. Future research should consider a greater number of realistic weathering cycles on multilayer wall systems with ACM than the three wetting and drying cycles considered here. Similarly, other ACMs should be tested to determine whether the observed phenomenon applies to several products than the one studied here. If so, the internal structure of ACMs deserves attention as it could be a cause for their increasing water absorptivity.

5. Conclusions

The water absorptivity of an aerogel-based coating mortar exposed to three subsequent wetting and drying cycles was studied using standardized laboratory measurements. The results showed that the capillary water absorptivity of the tested samples increased repeatedly after each wetting and drying cycle. The water absorptivity was more than five times higher in the third cycle than in the first cycle, although the increasing rate was reduced between the second and third cycle. The observed phenomenon could potentially indicate an unstable performance of the material through its service life and increase the uncertainties of the moisture risk assessment analyses. Future research is needed to investigate the consequence of the observed increasing water absorptivity of the aerogel-based coating mortar when applied in field, the reasons behind the observed phenomenon and if it is applicable to other aerogel-based coating mortars.

References

[1] Karim A N, Johansson P and Sasic Kalagasidis A 2022 Knowledge gaps regarding the hygrothermal and long-term performance of aerogel-based coating mortars *Constr. Build. Mater.* **314** 125602

[2] Kottek M, Grieser J, Beck C, Rudolf B and Rubel F 2006 World map of the Köppen-Geiger climate classification updated *Meteorol. Zeitschrift* **15** 259–63

[3] Frick J, Sakiyama N, Stipetic M and Garrecht H 2020 Large Scale Laboratory and Field Tests of Aerogel Renders *XVInternational Conference on Durability of Building Materials and Components* (Barcelona)

[4] Sakiyama N R M, Frick J, Stipetic M, Oertel T and Garrecht H 2021 Hygrothermal performance of a new aerogel-based insulating render through weathering: Impact on building energy efficiency *Build. Environ.* **202** 108004
[5] Maia J, Pedroso M, Ramos N M M, Flores-Colen I, Pereira P F and Silva L 2021 Durability of a New Thermal Aerogel-Based Rendering System under Distinct Accelerated Aging Conditions *Mater. 2021, Vol. 14, Page 5413* **14** 5413
[6] Berardi U and Nosrati R H 2018 Long-term thermal conductivity of aerogel-enhanced insulating materials under different laboratory aging conditions *Energy* **147** 1188–202
[7] Nosrati R and Berardi U 2017 Long-term performance of aerogel-enhanced materials *Energy Procedia* **132** 303–8
[8] Morgado A, Soares A, Flores-Colen I, Veiga M do R and Gomes M G 2021 Durability of Thermal Renders with Lightweight and Thermal Insulating Aggregates: Regranulated Expanded Cork, Silica Aerogel and Expanded Polystyrene *Gels 2021, Vol. 7, Page 35* **7** 35
[9] de Fátima Júlio M, Soares A, Ilharco L M, Flores-Colen I and de Brito J 2016 Aerogel-based renders with lightweight aggregates: Correlation between molecular/pore structure and performance *Constr. Build. Mater.* **124** 485–95
[10] Pedroso M, Flores-Colen I, Silvestre J D, Gomes M G, Silva L, Sequeira P and de Brito J 2020 Characterisation of a multilayer external wall thermal insulation system. Application in a Mediterranean climate *J. Build. Eng.* **30** 101265
[11] Soares A, de Fátima Júlio M, Flores-Colen I, Ilharco L M and Brito J de 2018 EN 998-1 performance requirements for thermal aerogel-based renders *Constr. Build. Mater.* **179** 453–60
[12] Flores-Colen I, Pedroso M, Soares A, Gomes M da G, Ramos N M M R, Maia J, Sousa R, Sousa H and Silva L 2020 In-Situ Tests on Silica Aerogel-Based Rendering Walls *XV International Conference on Durability of Building Materials and Components* (Barcelona)
[13] Maia J, Pedroso M, Ramos N M M, Pereira P F, Flores-Colen I, Glória Gomes M and Silva L 2021 Hygrothermal performance of a new thermal aerogel-based render under distinct climatic conditions *Energy Build.* **243** 111001
[14] Pedroso M, Flores-Colen I, Silvestre J D, Gomes M G, Silva L and Ilharco L 2020 Physical, mechanical, and microstructural characterisation of an innovative thermal insulating render incorporating silica aerogel *Energy Build.* **211** 109793
[15] Ibrahim M, Wurtz E, Biwole P H, Achard P and Sallee H 2014 Hygrothermal performance of exterior walls covered with aerogel-based insulating rendering *Energy Build.* **84** 241–51
[16] European Committee for Standardization (CEN) 2002 *EN 1015-18 Methods of test for mortar for masonry – Part 18: Determination of water absorption coefficient due to capillary action of hardened mortar*
[17] European Committee for Standardization (CEN) 2016 *EN 998-1 Specification for mortar for masonry – Part 1: Rendering and plastering mortar*
[18] Wall systems 2022 HECK AERO iP